(12) INTERNATIONAL APPLICATION PUBLISHED UNDER THE PATENT COOPERATION TREATY (PCT)

(19) World Intellectual Property Organization
International Bureau

(43) International Publication Date
4 September 2008 (04.09.2008)

PCT

(10) International Publication Number
WO 2008/106507 A2

(51) International Patent Classification:
A61K 48/00 (2006.01)

(21) International Application Number:
PCT/US2008/055116

(22) International Filing Date:
27 February 2008 (27.02.2008)

(25) Filing Language: English

(26) Publication Language: English

(30) Priority Data:
60/891,829 27 February 2007 (27.02.2007) US

(71) Applicant *(for all designated States except US)*: **UNIVERSITY OF SOUTH FLORIDA** [US/US]; 3802 Spectrum Blvd., Ste. 100, Tampa, Florida 33612 (US).

(72) Inventors; and

(75) Inventors/Applicants *(for US only)*: **CHEN, Jiandong** [US/US]; 19123 Autumn Woods Ave., Tampa, Florida 33647 (US). **HU, Baoli** [CN/US]; 4504 Blue Tee Ct., Apt. 70, Tampa, Florida 33613 (US).

(74) Agent: **HOPEN, Anton J.**; 180 Pine Avenue North, Oldsmar, Florida 34677 (US).

(81) Designated States *(unless otherwise indicated, for every kind of national protection available)*: AE, AG, AL, AM, AO, AT, AU, AZ, BA, BB, BG, BH, BR, BW, BY, BZ, CA, CH, CN, CO, CR, CU, CZ, DE, DK, DM, DO, DZ, EC, EE, EG, ES, FI, GB, GD, GE, GH, GM, GT, HN, HR, HU, ID, IL, IN, IS, JP, KE, KG, KM, KN, KP, KR, KZ, LA, LC, LK, LR, LS, LT, LU, LY, MA, MD, ME, MG, MK, MN, MW, MX, MY, MZ, NA, NG, NI, NO, NZ, OM, PG, PH, PL, PT, RO, RS, RU, SC, SD, SE, SG, SK, SL, SM, SV, SY, TJ, TM, TN, TR, TT, TZ, UA, UG, US, UZ, VC, VN, ZA, ZM, ZW.

(84) Designated States *(unless otherwise indicated, for every kind of regional protection available)*: ARIPO (BW, GH, GM, KE, LS, MW, MZ, NA, SD, SL, SZ, TZ, UG, ZM, ZW), Eurasian (AM, AZ, BY, KG, KZ, MD, RU, TJ, TM), European (AT, BE, BG, CH, CY, CZ, DE, DK, EE, ES, FI, FR, GB, GR, HR, HU, IE, IS, IT, LT, LU, LV, MC, MT, NL, NO, PL, PT, RO, SE, SI, SK, TR), OAPI (BF, BJ, CF, CG, CI, CM, GA, GN, GQ, GW, ML, MR, NE, SN, TD, TG).

Published:

— *without international search report and to be republished upon receipt of that report*

[Continued on next page]

(54) Title: MDM2/MDMX INHIBITOR PEPTIDE

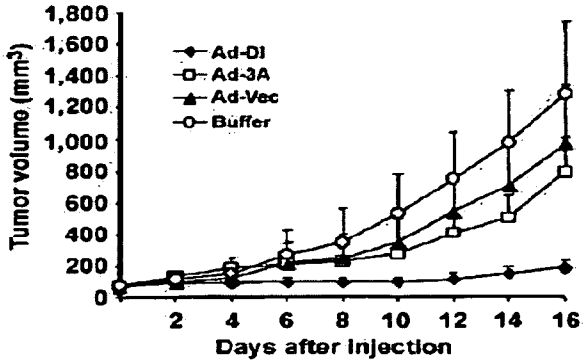

Figure 20.

(57) **Abstract:** The present invention relates to the use of dual inhibitor of p53 regulatory proteins to selectively inhibit neoplastic growth and induce apoptosis in unregulated cells. A novel peptide that inhibits p53 interactions with MDM2 and MDMX was identified and inserted into a virus nucleic acid sequence to serve as a cell-permeable activator of the p53 tumor suppressor protein. The invention also provides a method of treating cancer by administering a dual-specific inhibitor MDM2/MDMX inhibitory protein into p53+ cancer cells. Administration of the MDM2/MDMX-inhibitory adenovirus is shown to induce cell cycle arrest and apoptosis in a p53-dependent manner.

WO 2008/106507 A2

— *with sequence listing part of description published separately in electronic form and available upon request from the International Bureau*

MDM2/MDMX INHIBITOR PEPTIDE

CROSS REFERENCE TO RELATED APPLICATION

This application claims priority to currently pending U.S. Provisional Patent Application No. 60/891,829, entitled "MDM2 and MDMX Dual-Specific Inhibitory Peptide", filed on 27 February, 2007, the contents of which are herein incorporated by reference.

GOVERNMENT SUPPORT

This invention was made with government support under CA094851 and CA109636 awarded by the National Institutes of Health. The government has certain rights in the invention.

FIELD OF INVENTION

This invention relates to inhibitor peptides. Specifically, the p53 inhibitory proteins MDM2 and MDMX are targeted to induce p53-dependent cellular responses or apoptosis.

BACKGROUND OF THE INVENTION

MDM2 is an ubiquitin E3 ligase for p53 and an important regulator of p53 stability and activity by forming a negative feedback loop (Levine AJ. p53, the cellular gatekeeper for growth and division. Cell 1997;88(3):323-31). Overexpression of MDM2 abrogates the ability of p53 to induce cell cycle arrest and apoptosis (Chen J, Wu X, Lin J, Levine AJ. mdm-2 inhibits the G1 arrest and apoptosis functions of the p53 tumor suppressor protein. Mol Cell Biol 1996;16(5):2445-52). In about 30% of human osteogenic sarcomas and soft tissue sarcomas, MDM2 is overexpressed due to gene amplification. In tumors without MDM2 amplification, hyperactivation of MDM2 due to silencing of ARF expression also leads to p53 inactivation. Therefore, MDM2 is a key factor in tolerance of wild-type p53 in nearly 50% of tumors, making it an attractive target for the development of novel anti-tumor agents.

The MDM2 homolog MDMX also binds to p53 and inhibits p53-dependent transcription (Shvarts A, Steegenga WT, Riteco N, et al. MDMX: a novel p53-binding protein with some functional properties of MDM2. Embo J 1996;15(19):5349-57). Loss of MDM2 or MDMX leads to embryonic lethality, which can be rescued by deletion of p53 (Jones SN, Roe AE, Donehower LA, Bradley A. Rescue of embryonic lethality in Mdm2-deficient mice by absence of p53. Nature 1995;378(6553):206-8; Montes de Oca Luna R, Wagner DS, Lozano G. Rescue of early embryonic lethality in mdm2-deficient mice by deletion of p53. Nature 1995;378(6553):203-6; Parant J, Chavez-Reyes A, Little NA, et al. Rescue of embryonic

lethality in Mdm4-null mice by loss of Trp53 suggests a nonoverlapping pathway with MDM2 to regulate p53. Nat Genet 2001;29(1):92-5). Therefore, expression of MDM2 and MDMX are both necessary for regulation of p53 during development. Unlike MDM2, MDMX does not have significant intrinsic E3 ligase activity (Stad R, Little NA, Xirodimas DP, et al. Mdmx stabilizes p53 and Mdm2 via two distinct mechanisms. EMBO Rep 2001;2(11):1029-34). However, MDMX forms heterodimers with MDM2 through COOH-terminal RING domain interactions which stimulates the ability of MDM2 to ubiquitinate and degrade p53 (Tanimura S, Ohtsuka S, Mitsui K, Shirouzu K, Yoshimura A, Ohtsubo M. MDM2 interacts with MDMX through their RING finger domains. FEBS Lett 1999;447(1):5-9; Sharp DA, Kratowicz SA, Sank MJ, George DL. Stabilization of the MDM2 oncoprotein by interaction with the structurally related MDMX protein. J Biol Chem 1999;274(53):38189-96; Gu J, Kawai H, Nie L, et al. Mutual dependence of MDM2 and MDMX in their functional inactivation of p53. J Biol Chem 2002;277(22):19251-4). Another consequence of MDMX-MDM2 heterodimer formation is that MDMX can be ubiquitinated and degraded by MDM2 (Pan Y, Chen J. MDM2 promotes ubiquitination and degradation of MDMX. Mol Cell Biol 2003;23(15):5113-2; Kawai H, Wiederschain D, Kitao H, Stuart J, Tsai KK, Yuan ZM. DNA damage-induced MDMX degradation is mediated by MDM2. J Biol Chem 2003;278(46):45946-53 de Graaf P, Little NA, Ramos YF, Meulmeester E, Letteboer SJ, Jochemsen AG. Hdmx protein stability is regulated by the ubiquitin ligase activity of Mdm2. J Biol Chem 2003;278(40):38315-24), this is an important mechanism for controlling MDMX level during p53 stress response.

Recent studies suggest that the major mechanism of p53 regulation by MDMX is the formation of inactive p53-MDMX complexes. Under non-stress conditions, MDM2 and p53 have short half-lives whereas MDMX is relatively stable. Therefore, elimination of MDMX is important for efficient p53 activation during stress response. DNA damage induces MDMX phosphorylation by ATM and Chk2 at several COOH-terminal serine residues (Ser^{342}, Ser^{367}, and Ser^{403}) generating a docking site for 14-3-3. These modifications stimulate MDMX degradation by MDM2, which facilitates p53 activation (Okamoto K, Kashima K, Pereg Y, et al. DNA damage-induced phosphorylation of MdmX at serine 367 activates p53 by targeting MdmX for Mdm2-dependent degradation. Mol Cell Biol 2005;25(21):9608-20; LeBron C, Chen L, Gilkes DM, Chen J. Regulation of MDMX nuclear import and degradation by Chk2 and 14-3-3. Embo J 2006;25(6):1196-206). Ribosomal stress resulting from disruption of rRNA biogenesis also activates p53 in part by promoting MDMX degradation through L11-MDM2 binding which enhances MDMX ubiquitination. MDMX overexpression leads to sequestration of p53 into inactive complexes and abrogates p53-mediated cell cycle arrest in response to ribosomal stress.

MDMX overexpression has been found in 40% of tumor cell lines, and in breast, colon, and lung tumor samples with 18.5% frequency. It is amplified in 4% of glioblastomas and 5% of breast tumors. More recently, approximately 60% of retinoblastomas have been found to have MDMX overexpression or gene amplification. MDMX overexpression prevents oncogenic ras-induced premature senescence in mouse fibroblasts and cooperates with activated ras to confer tumorigenic potential in nude mice (Danovi D, Meulmeester E, Pasini D, et al. Amplification of Mdmx (or Mdm4) directly contributes to tumor formation by inhibiting p53 tumor suppressor activity. Mol Cell Biol 2004;24(13):5835-43). RNAi-mediated knockdown of MDMX in HCT116 tumor cells suppresses tumor xenograft formation in nude mice (Gilkes DM, Chen L, Chen J. MDMX regulation of p53 response to ribosomal stress. Embo J 2006;25(23):5614-25). Because MDM2 and MDMX overexpression or deregulation mainly occurs in tumors that retain wild-type p53, they are appealing targets for cancer drug discovery.

The extensive validation of MDM2 as a drug target resulted in the development of Nutlin, which can activate p53 by disrupting p53-MDM2 complex in tumor cells and tumor xenograft models. MDM2 and MDMX showed ~50% amino acid sequence identity in their p53-binding domains. However, recent studies reveal that Nutlin is inefficient for disruption of MDMX-p53 interaction and failed to activate p53 in cells overexpressing MDMX. Knockdown of MDMX cooperates with Nutlin to activate p53 in tumor cells and induces growth arrest. These results suggest that development of novel inhibitors optimized for dual-inhibition of MDM2 and MDMX are necessary to achieve full activation of p53.

SUMMARY OF INVENTION

The present invention relates to the finding that dual inhibition of p53 regulatory proteins selectively inhibits neoplastic growth and induces apoptosis in tumor cells.

A phage display technique was used to identify a novel peptide that can inhibit p53 interactions with MDM2 (IC_{50}=10 nM) and MDMX (IC_{50}=100 nM). This peptide was found to act as a dual specific inhibitor of both MDM2 and MDMX. The thioredoxin coding region with the MDM2/MDMX inhibitory peptide insert was constructed and clones into a plasmid vector (Stratagene). The plasmid was linearized and cotransformed into *E. coli* with adenoviral backbone plasmid, and the recombined adenovirus genome wa purified and transfected into AD-293 cells to generate adenoviruses that express the Flag epitope tagged thioredoxin-inhibitory peptide fusion protein.

In one embodiment, expression of the thioredoxin scaffold protein displaying this peptide sequence by recombinant adenovirus for the first time achieved disruption of both MDM2 and

MDMX interaction with p53, resulting in efficient p53 activation and apoptosis of MDMX-overexpressing tumor cells in culture and in mice in a p53-dependent fashion.

The invention also provides a method of treating cancer by administering a MDM2/ MDMX inhibitory compound into $p53^+$ cancer cells. Inhibitory compounds must be identified that inhibit p53-MDM2 and p53-MDMX interactions, which may include using a phage display method. After cancer cells with wild-type p53 are identified, the cells are treated with the MDM2/ MDMX inhibitory compound. The inhibitory compound can be a nucleic acid or polypeptide, and is preferably a dual specific inhibitor of MDM2 and MDMX. Additionally, the compound may be a fusion protein. Preferably, the compound is inserted into a viral vector for administration.

BRIEF DESCRIPTION OF THE DRAWINGS

For a fuller understanding of the invention, reference should be made to the following detailed description, taken in connection with the accompanying drawings, in which:

FIG. 1 is a table of the peptide sequence results selected by the phage display.

FIG. 2 is a graph depicting the phage display-selected pDI (SEQ. ID. No. 1) and control p3A peptides, tested in an ELISA assay of GST-MDM2 binding to immobilized His6-p53.

FIG. 3 is a graph depicting the phage display-selected pDI (SEQ. ID. No. 1) and control p3A peptides, tested in an ELISA assay of GST-MDMX binding to immobilized His6-p53.

FIG. 4 is a table depicting the inhibition of MDM2- and MDMX-p53 binding by peptides in ELISA.

FIG. 5 depicts the ability of DI peptide to disrupt p53 binding to both MDM2 and MDMX. Glutathione beads were loaded with GST-p53-1-52 fusion protein and incubated with a mixture of *in vitro* translated MDM2 and MDMX and different concentrations of DI. Binding of MDM2 and MDMX to GST-p53-1-52 in the presence of inhibitors was determined by autofluorography after washing and SDS-PAGE.

FIG. 6 depicts the ability of Nutlin to disrupt p-53-MDM2 binding but not p-53-MDMX binding. Glutathione beads were loaded with GST-p53-1-52 fusion protein and incubated with a mixture of *in vitro* translated MDM2 and MDMX and different concentrations of Nutlin. Binding of MDM2 and MDMX to GST-p53-1-52 in the presence of inhibitors was determined by autofluorography after washing and SDS-PAGE.

FIG. 7 is a schematic representation of the scaffold protein *E. coli* thioredoxin with pDI (SEQ. ID. No. 1) and p3A inserted between Gly^{33} and Pro^{34} at the active center.

FIG. 8 is a schematic representation depicting the coding regions of Thioredoxin-DI and Thioredoxin-3A fused to FLAG epitope in the adenovirus genome. The cytomegalovirus (CMV) promoter drives expression of FLAG-DI or FLAG-3A and an IRES element allows co-expression of hrGFP from the same transcript.

FIG. 9 is a blot depicting Flag immunoprecipitates after cell infection. MCF-7 cells were infected with Ad-DI, Ad-3A and Ad-Vec (MOI=300) for 48 h and cell lysate was immunoprecipitated by FLAG antibody and blotted for coprecipitation of MDM2 and MDMX.

FIG. 10 is a blot depicting p53 immunoprecipitates after cell infection. MCF-7 cells were treated with Ad-DI, Ad-3A and Ad-Vec (MOI=300) or Nutlin (10 μM) for 48 h and MG132 (30 μM) was added 4 h before harvest. Cell lysate was immunoprecipitated by p53 antibody and blotted for coprecipitation of MDM2 and MDMX.

FIG. 11 is a blot depicting inhibition of MDM2 and MDMX-p53 binding by FLAG-DI activates p53. Cells were infected with the recombinant adenoviruses (MOI=100) for 48 h and analyzed by western blot.

FIG. 12 is a blot depicting inhibition of MDM2 and MDMX-p53 binding by FLAG-DI activates p53. Cells were infected with the recombinant adenoviruses (MOI=100) for 48 h and analyzed by western blot.

FIGS. 13(A) and (B) are graphs depicting inhibition of MDM2 and MDMX-p53 binding by FLAG-DI activates p53. (A) HCT116 and (B) MCF-7 cells stably transfected with p53-responsive BP100-luc reporter plasmid were infected with Ad-DI at the indicated MOI for 48 h and luciferase activity was determined (n=3).

FIGS. 14(A) and (B) are graphs depicting inhibition of MDM2 and MDMX-p53 binding by FLAG-DI activates p53. HCT116-$p53^{+/+}$ and HCT116-$p53^{-/-}$ cells were infected with Ad-DI (MOI=300) for 48 h. (A) Reduction of S phase was analyzed by propidium iodide staining and FACS. (B) Apoptosis was measured by the level of sub-G1 fraction in FACS analysis.

FIG. 15 is a graph showing p53 activation in MDM2- and MDMX-overexpressing cells following FLAG-DI treatment. JEG3 and Y79 cells were treated with Ad-DI (MOI=300) or Nutlin (10 μM) for 48 h and analyzed by FACS for apoptotic sub-G1 population.

FIGS. 16(A) and (B) are blots depicting activation in MDM2- and MDMX-overexpressing cells following FLAG-DI treatment. U2OS expressing inducible (A) MDMX (Tet-on) and (B) MDM2 (Tet-off) were treated with 0.1 μg/ml tetracycline for 18 h, followed by treatment with Ad-DI (MOI=100) or Nutlin (10 μM) for additional 24 h, and p53 activation markers were analyzed by western blot.

FIG. 17 is a graph showing p53 activation in MDM2- and MDMX-overexpressing cells following FLAG-DI treatment. U2OS and U2OS-MDMX cells were treated with Ad-DI (MOI=300) and Nutlin (10 μM) for 48 h and analyzed by FACS for sub-G1 population.

FIGS. 18(A) and (B) are graphs depicting activation in MDM2- and MDMX-overexpressing cells following FLAG-DI treatment. (A) U2OS and (B) U2OS-MDMX cells were treated with Ad-DI and Nutlin at indicated concentrations for 5 days and analyzed by MTT assay for cell viability.

FIG. 19 is a blot showing the cellular effects of recombinant adenovirus on peptide epitode expression. HCT116-$p53^{+/+}$ cells were infected with Ad-DI (MOI=100) or treated with doxorubicin (2 μM), etoposide (10 μM) for 24h. The amount of total p53 and phosphorylated p53 (Ser^{15}) was determined by Western blot.

FIG. 20 is a graph showing the tumor growth and anticancer activity of Ad-DI. Nude mice bearing HCT116-$p53^{+/+}$ xenografts were treated with Ad-DI, Ad-3A, Ad-Vector or buffer by 5 consecutive daily intra-tumoral injections (5×10^{10} PFU/injection). The tumor volumes were measured every two days after completion of treatment cycle.

FIG. 21 is a blot showing the anticancer activity of Ad-DI. Representative tumor samples recovered 48 h after injection were lysed and protein expression levels analyzed by western blot.

FIGS. 22(A) through (D) are images of tumor speciments 48 h after injection with either Ad-DI or Ad-3A. The cells were stained for p53 and FLAG in serial sections.

FIGS. 23 (A) and (B) are graphs showing the anticancer activity of Ad-DI. HCT116-$p53^{-/-}$ and HCT116-MDMX tumor xenografts were treated with intra-tumoral injection of 5×10^{10} Ad-DI or Ad-3A for 5 consecutive days. Tumor growth was measured for the indicated time frame after completion of injections.

DETAILED DESCRIPTION OF THE PREFERRED EMBODIMENT

The term"cancer" is used throughout the specification to identify a disease characterized by neoplastic events or other abonormal cellular proliferation occurring in biological organisms. Such neoplastic events include oncogenesis and include carcinomas, sarcomas, leukemias, lymphomas, myelomas, and central nervous system cancers.

The term "fusion protein" is used throughout the specification to identify a protein resulting from joining two or more genes which originally encoded separate proteins. The protein is created by joining the coding regions of one gene in frame with a second gene, resulting in transcription of both genes. Upon translation, the resultant protein possesses properties from each gene.

The term "MDM2" is used throughout the specification to identify the cellular protein encoded by the MDM2 gene. MDM2 is a critical E3 ubiquitin ligase of p53 and inhibitor of p53 transcription and contains RING finger ubiquitin ligase domain. MDM2 functions by mediating the ubiquination of p53 and is capable of autoubiquination. MDM2 also interacts with MDMX and promotes MDMX degradation.

The term "MDMX" is used throughout the specification to identify the cellular protein homologue of MDM2, encoded by the MDMX gene. MDMX is a negative regulator of p53 by binding p53 and also interacts with MDM2 to affect MDM2's function. Addition of MDMX to in vitro ubiquitination assays containing MDM2 results in a synergistic increase of ubiquitin conjugation to MDM2.

The term "nucleic acid" is used throughout the specification to identify cellular and viral genetic material comprising chains of nucleotides, including deoxyribonucleic acid and ribonucleic acid.

The term "polypeptide" is used throughout the specification to identify cellular combinations of amino acids, attached via peptide bonds, and include proteins.

The term "reporter gene" is used throughout the specification to identify a gene that is attached to a second gene, which is a gene of interest in an investigation. The reporter gene permits easy identification of a fusion protein, and may contain selectable properties allowing, for example, fluorescent marker attachment.

The term "specific inhibitor" is used throughout the specification to identify a composition that reduces the activity level or levels of a protein of interest to a greater extent than it reduces the activity levels of other cellular proteins.

The term "virus nucleic acid sequence" is used throughout the specification to identify viral genetic material, either as deoxyribonucleic acid or ribonucleic acid sequences.

The following provides examples and guidance for carrying out the various aspects of the present invention.

ELISA Assay

GST-MDM2-1-150 and GST-MDMX-1-200 containing human MDM2 and MDMX, and His6-tagged human p53 expressed in *E. coli* were used in ELISA as described previously (Hu B, Gilkes DM, Farooqi B, Sebti SM, Chen J. MDMX overexpression prevents p53 activation by the MDM2 inhibitor Nutlin. J Biol Chem 2006;281(44):33030-5).

GST pull down assay

^{35}S-methionine-labeled MDMX and MDM2 were generated using the TNT *in vitro* transcription/translation kit (Promega). Five micro liters of the translation products were mixed and incubated with glutathione-agarose beads loaded with 5 µg GST-p53-1-52 in lysis buffer [50 mM Tris-HCl (pH 8.0), 5 mM EDTA, 150 mM NaCl, 0.5% Nonidet P-40, 1 mM phenylmethylsulfonyl fluoride] for 2 h at 4 °C. The beads were washed with lysis buffer, fractionated by SDS-PAGE, and bound MDMX and MDM2 were detected by auto fluorography.

Cell lines and antibodies

Tumor cell lines H1299 (lung, p53-null), U2OS (bone), MCF-7 (breast), JEG-3 (placenta), DLD-1 (breast) were maintained in DMEM medium with 10% fetal bovine serum. HCT116-p53$^{+/+}$ and HCT116-p53$^{-/-}$ cells were kindly provided by Dr. Bert Vogelstein. Retinoblastoma Y79 cell line was provided by Dr. George Blanck. Normal human skin fibroblast HFF was provided by Dr. Jack Pledger. The U2OS stable cell line with MDMX overexpression, and U2OS stable cell line expressing tetracycline- regulated human MDM2 and MDMX were previously described (Pan Y, Chen J. MDM2 promotes ubiquitination and degradation of MDMX. Mol Cell Biol 2003;23(15):5113-21; Hu B, Gilkes DM, Farooqi B, Sebti SM, Chen J. MDMX overexpression prevents p53 activation by the MDM2 inhibitor Nutlin. J Biol Chem 2006;281(44):33030-5). The following antibodies were used in the experiment: 3G9 (mouse) and a rabbit polyclonal serum for MDM2 western blot and IP; DO-1 (Pharmingen) and FL393 (Santa Cruz) for p53 western blot; 8C6 monoclonal or a rabbit polyclonal serum for MDMX western blot and IP; anti-p21WAF (Santa Cruz) for p21. P53 ubiquitination assay was performed as described previously (Pan Y, Chen J. MDM2 promotes ubiquitination and degradation of MDMX. Mol Cell Biol 2003;23(15):5113-21).

Animal studies

Athymic-NCr-nu female mice between 7 and 8 weeks were inoculated subcutaneously on both flanks with 5×10^6 HCT116 cells. Tumor formation was followed for 4-6 days. When tumor size reached ~0.2 cm^3, the mice were injected with 5 $\times10^{10}$ PFU of Ad-DI or control adenoviruses every day for a total of five times. Tumor volume was calculated with the formula: $[(\text{length+width})/2]^3 \times 0.5236$. Tumors recovered after termination of the experiments were fixed in formalin and paraffin sections were analyzed by immunohistochemical staining using rabbit antibodies against p53 and FLAG.

Identification of MDM2/MDMX inhibitory peptide

Novel peptide inhibitors of MDM2 and MDMX were identified using a phage display to screen a 12-mer library to obtain peptides that bind to the p53-binding domains of MDM2 and MDMX. The phage display was created from an M13 phage library (Ph.D.-12, New England Biolabs) encoding random 12-mer peptides at the N-terminus of pIII coat protein (2.7×10^9 sequences). GST-MDM2-1-150 and GST-MDMX-1-200 fusion proteins containing the p53 binding domain of human MDM2 and MDMX were expressed in *E. coli* and loaded onto glutathione-agarose beads. The loaded beads were incubated with blocking buffer (0.1 M $NaHCO_3$, PH 8.6, 5 mg/ml BSA, 0.02% NaN_3) for 1 h at 4 ℃, washed with TBST (50 mM Tris, pH 7.5, 150 mM NaCl, 0.1% Tween 20), and incubated in TBST at 4 ℃ with 4×10^{10} phages. Bound phages were eluted with 0.2 M glycine, pH 2.2, 1 mg/ml BSA and neutralized with 1 M Tris, pH 9.1. The eluted phages were amplified as instructed by the manufacturer. The binding/amplification process was repeated 4 cycles for both targets. Phage DNA was prepared and the region of interest was sequenced. The results showed that 7/10 MDMX-selected and 4/10 MDM2-selected phages contain the same insert LTFEHYWAQLTS (SEQ. ID. No. 1), as seen in Figure 1. This peptide was named pDI for peptide Dual Inhibitor. The remaining phages contain unrelated and inactive sequences when tested by ELISA and were not characterized further.

The results indicated that screens using GST-MDM2 or GST-MDMX resulted in the selection of the same peptide, suggesting pDI (SEQ. ID. No. 1) has such high affinity for both MDM2 and MDMX that it out-competed any potential isoform-specific peptides by a significant margin. The pDI peptide (LTFEHYWAQLTS) (SEQ. ID. No. 1) is distinct from the p53 peptide (16-QETFSDLWKLLP-28) and the previously identified 12/1 peptide (MPRFMDYWEGLN) that interacts with MDM2 and MDMX, but retains 3 key p53 hydrophobic residues (Phe19, Trp23, and Leu26, underlined) that contact the MDM2 pocket. In an ELISA assay, pDI (SEQ. ID. No. 1) inhibited MDM2-p53 and MDMX-p53 interactions with IC_{50} of 10 and 100 nM respectively, which is 15, 60, and 300-fold better than 12/1, Nutlin, and p53 peptide on

MDM2. See Figures 2 through 4). Mutation of the 3 key hydrophobic residues to alanine (p3A) abrogated MDM2 and MDMX inhibition, suggesting that pDI (SEQ. ID. No. 1) mimics p53 binding to MDM2 and MDMX. In a different assay, pDI (SEQ. ID. No. 1) also inhibited GST-p53 capture of *in vitro* translated MDM2 and MDMX with different efficiency, as seen in Figure 5. In contrast, Nutlin only blocked MDM2 but had no effect on MDMX-p53 interaction, depicted in Figure 6. The 10-fold difference in IC_{50} for MDM2 and MDMX suggests that MDMX may bind p53 with higher affinity than MDM2, which is consistent with its mechanism of p53 inhibition by sequestration.

A method to deliver the pDI peptide (SEQ. ID. No. 1) into cells

After unsuccessful attempts to activate p53 in cells by fusion or conjugation of pDI (SEQ. ID. No. 1) to the Antennapedia cell-permeable peptide, the pDI sequence (SEQ. ID. No. 1) was inserted into the active center of FLAG-tagged *E. coli* thioredoxin reporter protein, that serves as a display scaffold. See Figure 7. Double stranded oligonucleotide (5'-GTCCGCCTCTGAGTTT GACGTTTGAGCATTATTGGGCGCAGTTGACGTCGGAAAACG) encoding pDI (SEQ. ID. No. 1), or a control p3A (Ad-3A) sequence, was cloned into the RsrII site of pBAD/Thio vector (Invitrogen). The complete thioredoxin coding region with the peptide insert was amplified by PCR (using 5'-GGTCGACCCATGGGATCTGATAAAATTATTCATC, 5'-GCTCGA GGGCCAGGTTAGCGTCG primers), cleaved with SalI and XhoI, and cloned into pShuttle-IRES-hrGFP-1 vector (Stratagene). The plasmid was linearized with PmeI and cotransformed into *E. coli* BJ5183 with adenoviral backbone plasmid pAdEasy-1. Recombinant plasmids were linearized with PacI and transfected into AD-293 cells (Stratagene) to generate viruses. Recombinant adenoviruses were purified by ultra centrifugation on $CsCl_2$ gradients and titered using the Adeno-X™ Rapid Titer Kit (Clontech). See Figure 8. The fusion proteins expressed in infected cells showed diffused cytoplasmic and nuclear staining consistent with their small sizes (~15 kd), and has a half life of ~1 hour which was unrelated to MDM2 binding (data not shown).

pDI (SEQ. ID. No. 1) was selected based on its ability to bind MDM2 and MDMX. To test whether insertion of pDI sequence (SEQ. ID. No. 1) into thioredoxin conferred the ability to bind MDM2 and MDMX, cells infected with Ad-DI virus were immunoprecipitated using FLAG antibody and analyzed for the coprecipitation of endogenous MDM2 and MDMX. The results showed that the FLAG-DI protein, but not FLAG-3A, coprecipitated with both MDM2 and MDMX when expressed in MCF7 cells. See Figure 9. Furthermore, FLAG-DI expression disrupted MDM2-p53 and MDMX-p53 coprecipitations, seen in Figure 10. Nutlin failed to disrupt MDMX-p53 complex in the same assay. Infection with Ad-DI did not cause p53 Ser^{15} phosphorylation, as seen in Figure 19, suggesting that the fusion protein disrupted p53

binding to MDM2 and MDMX by a competitive mechanism without triggering DNA damage signaling. These results demonstrated that the FLAG-DI fusion protein was expressed at levels sufficient to compete with p53 for binding to endogenous MDM2 and MDMX.

Example 1

Assuming MDM2 and MDMX ubiquinate p53, disruption of p53-MDM2 and p53-MDMX complexes should result in p53 stabilization and activation. In fact, infection of tumor cells or normal human foreskin fibroblasts expressing wild type p53 with Ad-DI resulted in significant increase in p53 level and induction of p53 targets (p21, MDM2, PUMA). See Figures 11 and 12. The effects were not observed using Ad-3A or Ad-vector control viruses, indicating that they were dependent on the pDI sequence (SEQ. ID. No. 1) in the fusion protein. Infection of p53 null (HCT116-$p53^{-/-}$) or mutant (DLD1) cell lines failed to induce p53 target genes, indicating that the effect of Ad-DI was p53-dependent, as seen in Figures 11 and 12. RT-PCR analysis indicated the increase in p21 and MDM2 levels was associated with an increase in mRNA (data not shown). Ad-DI infection also activated a stably integrated p53-responsive reporter, BP100-luc, in HCT116 and MCF7 cells, see Figure 13, indicating activation of p53 transcriptional function. Ad-DI infection inhibited p53 ubiquitination by MDM2 (data not shown), consistent with its ability to disrupt MDM2-p53 binding. Cell cycle analysis by FACS revealed about 10-fold reduction of S-phase population in the Ad-DI infected HCT116-$p53^{+/+}$ cells but not in HCT116-$p53^{-/-}$ cells, seen in Figures 14(A) and 14(B). Ad-DI infection also induced significant apoptosis in HCT116-53+/+ cells, but was much less effective in HCT116-$p53^{-/-}$ cells, as seen in Figures 14(A) and 14(B). Therefore, the cell cycle arrest and apoptosis activities of Ad-DI are mediated by activation of p53.

Example 2

Ad-DI's p53-activating efficiency was tested in cells overexpressing high levels of MDM2 and MDMX overexpression. Nutlin does not disrupt MDMX-p53 binding when applied at practical concentrations dictated by solubility and non-specific toxicity (5-10 μM). Futher, p53 activation by Nutlin is attenuated in cells overexpressing MDMX. To determine if Ad-DI is more efficient in activating p53 in cells overexpressing MDMX, JEG3 (high MDM2 and MDMX) and Y79 (high MDMX) cells were treated with the virus. The results showed that Ad-DI infection resulted in significant apoptosis in both cell lines, whereas Nutlin was considerably less effective, as seen in Figure 15. These results suggested that FLAG-DI is able to overcome physiological levels of MDM2 and MDMX overexpression.

To further test FLAG-DI's ability to overcome high levels of MDM2 and MDMX overexpression, U2OS cells expressing tetracycline-regulated MDM2 (~8x endogenous level)

and MDMX (~8x endogenous level) were treated with Ad-DI and Nutlin. The results showed that Nutlin remained highly effective even when MDM2 is overexpressed, whereas MDMX overexpression completely abrogated the ability of Nutlin to activate p53. See Figures 16(A) and 16(B). In contrast, the activity of Ad-DI was only moderately inhibited by MDM2 and MDMX overexpression, consistent with a competitive mechanism of FLAG-DI action. Additional assays using U2OS with further MDMX overexpression (30x endogenous level, non-inducible) also demonstrated the ability of Ad-DI to activate p53 under conditions when Nutlin was completely ineffective (data not shown). FACS and MTT assays show Ad-DI induced significant apoptosis in the U2OS-MDMX cells, which were completely resistant to Nutlin, as seen in Figures 17 through 18(B). Moreover, treatment of normal human foreskin fibroblasts (HFF) with Ad-DI did not cause apoptosis (data not shown). This is expected since most non-transformed cell types do not undergo apoptosis upon p53 activation. These results suggested that FLAG-DI is an efficient activator of p53 in tumor cells overexpressing MDM2 and MDMX due to its ability to neutralize both proteins.

Example 3

To elucidate the effect of inhibiting MDM2 and MDMX, tumor cells or normal human skin fibroblasts expressing wild type p53 were infected with Ad-DI. The infection resulted in significant increase in p53 level and induction of p53 targets, including p21, MDM2, PUMA, as seen in Figures 12 and 13. However, the effects were not observed using Ad-3A or Ad-vector control viruses. Infection of p53 null (HCT116-$p53^{-/-}$) or mutant (DLD1) cell lines failed to induce p53 target genes, indicating that the effect of Ad-DI was p53-dependent. See Figures 12 and 13. Ad-DI infection also activated a stably transfected p53-responsive reporter BP100-luc in cell culture, as seen in Figure 13, indicating activation of p53 transcriptional function. P53 mRNA levels remained unchanged after Ad-DI infection, suggesting that the mechanism of p53 activation was due to stabilization (data not shown). Further, Ad-DI infection inhibited p53 ubiquitination by MDM2 (data not shown), consistent with its ability to disrupt MDM2-p53 binding. Infection with Ad-DI did not cause p53 Ser^{15} phosphorylation, seen in Figure 19, suggesting that the fusion protein activates p53 by competitive inhibition of MDM2 and MDMX, without triggering DNA damage signaling. Additionally, cell FACS cycle analysis revealed about 10-fold reduction in the S-phase population of Ad-DI infected HCT116-$p53^{+/+}$ cells but not in HCT116 $p53^{-/-}$ cells, as seen in Figure 14. Ad-DI infection also induced significant apoptosis in HCT116-$53^{+/+}$ cells, but was much less effective in HCT116 $p53^{-/-}$ cells, seen in Figure 14. Therefore, the cell cycle arrest and apoptosis activities of Ad-DI are mediated by activation of p53.

Example 4

To test the anti-tumor potential of Ad-DI, HCT116 tumor xenografts (~0.2 cm^3) were treated with daily single intra-tumoral injection of 5×10^{10} PFU Ad-DI or control virus for 5 consecutive days. This resulted in 90% suppression of tumor growth for the following 16 days by Ad-DI but not by control viruses or buffer, as seen in Figure 20. The difference in tumor suppression effects of Ad-DI (n=10), Ad-3A (n=6), Ad-Vector (n=8), and buffer (n=17) were statistically significant ($P<0.01$). Similar treatment of larger tumors (>0.5 cm^3) resulted in moderate growth inhibition in only a subset of animals (data not shown), most likely due to limited access of the virus to distant parts of the tumor. Strong induction of p53, MDM2 and p21 were observed in the extract of tumors 48 hours after injection with Ad-DI. See Figure 21. Induction of p53, MDM2 and p21 were observed in the extract of tumors injected with Ad-DI (data not shown). Immunohistochemical staining of tumor serial sections showed localized expression of FLAG-DI in the nucleus and cytoplasm of tumor cells near the sites of injection, which correlates with significant p53 staining in the same area as seen in Figures 22(A) through 22(C).

Consistent with cell culture results, the anti-tumor effect of Ad-DI was strictly dependent on p53. The growth of HCT116-$53^{-/-}$ tumor xenograft was not inhibited by Ad-DI (n=6) and Ad-3A (n=6, $P>0.05$). See Figure 23(A). Furthermore, Ad-DI also inhibited the growth of tumor xenograft formed by a modified HCT116-MDMX cell line overexpressing MDMX (~5 fold, Figure 23(B) ($P<0.01$, n=5), and induced p53 activation as determined by western blot and immunohistochemical staining (data not shown). Ad-DI and control viruses were well-tolerated in mice after intra-tumoral administration, with no observable weight loss or pathological changes of different organs (data not shown).

Recent studies suggest that MDM2 regulates p53 mainly by promoting its degradation, whereas MDMX acts by sequestration of p53. Although current understanding of the role of MDMX in cancer is still limited, cell culture experiments suggest MDMX is a significant player in suppressing p53 activity in at least a subset of tumors. Several studies of MDMX expression in clinical samples also strongly implicate its involvement in cancer development. These observations suggest a need to further evaluate the potential of MDMX as a therapeutic target. MDMX knockout and RNAi provided valuable evidence for the functional importance of MDMX in regulating p53. However, because MDMX also interacts with other molecules such as MDM2 and casein kinase 1, MDMX depletion does not provide the best simulation of disrupting MDMX-p53 binding.

The MDM2 inhibitor Nutlin was developed specifically for MDM2. Interestingly, Nutlin has been shown to be at least 30-fold less efficient in disrupting MDMX-p53 binding. When applied at practical concentrations, Nutlin is likely to function only by inhibiting MDM2. MDMX

is also insensitive to a class of small molecule MDM2 inhibitors that are α-helical mimics based on the terphenyl scaffold (unpublished results). These observations suggest that the p53-binding pockets on MDM2 and MDMX have differences that affect the binding of small molecules. Such differences may also compromise the effect of other small molecules optimized for MDM2.

For therapeutic applications, it is beneficial to have an inhibitor that is dual-specific for MDM2 and MDMX. The screening for MDM2 and MDMX binding peptides resulted in the identification of the same sequence motif. This finding suggests that MDM2 and MDMX have similar binding specificity to peptide sequences, which is distinct from their interactions with small molecules. It is possible that peptides rely on extensive contacts with the p53 binding pockets and is not sensitive to minor differences that affect small molecule ligands. Interestingly, in both ELISA and GST pull down assays, disruption of MDMX-p53 interaction always require ~10-fold higher concentrations of the pDI peptide (SEQ. ID. No. 1). This suggests that MDMX may bind p53 with higher affinity than MDM2, which is consistent with its mechanism of p53 inhibition by forming stable complexes.

Simultaneous inhibition of MDM2 and MDMX binding to p53 has strong pro-apoptotic potential in cell culture and can efficiently suppress tumor growth *in vivo*. The ability of Ad-DI to induce apoptosis is at significant contrast to Nutlin, which induces cell cycle arrest in most tumor cell lines. It is possible that FLAG-DI's ability to target both MDM2 and MDMX caused activation of p53 over the apoptotic threshold. The potent MDM2/MDMX dual inhibitor, pDI peptide (SEQ. ID. No. 1), provides a novel motif for structural study of MDM2 and MDMX interactions with a high affinity ligand and should aid the design of small molecule inhibitors.

The disclosure of all publications cited above are expressly incorporated herein by reference, each in its entirety, to the same extent as if each were incorporated by reference individually.

It is also to be understood that the following claims are intended to cover all of the generic and specific features of the invention herein described, and all statements of the scope of the invention which, as a matter of language, might be said to fall therebetween. Now that the invention has been described,

What is claimed is:

1. An inhibitory compound specific for inhibition of both MDM2 and MDMX, whereby cellular responses or apoptosis are induced.
2. The compound of claim 1, wherein p53-MDM2 and p53-MDMX interactions are inhibited.
3. The compound of claim 1, wherein the inhibitory compound is a nucleic acid or polypeptide.
4. The compound of claim 1, wherein the inhibitory compound is [SEQ ID NO: 1].
5. The compound of claim 1, wherein the inhibitory compound shares at least 85% sequence homology with [SEQ ID NO: 1].
6. The compound of claim 1, wherein the inhibitory compound is a nucleic acid that encodes [SEQ ID NO: 1].
7. The compound of claim 6, wherein the nucleic acid encodes a polypeptide having at least 85% sequence homology to [SEQ ID NO: 1].
8. The compound of claim 1, wherein the inhibitory compound is linked to a reporter gene.
9. The compound of claim 4, wherein the inhibitory compound is a component of a fusion protein.
10. The compound of claim 9, wherein the fusion protein contains a FLAG reporter gene.
11. The compound of claim 1, wherein the inhibitory compound is inserted into a virus nucleic acid sequence.
12. The compound of claim 11, wherein the virus is an adenovirus.
13. A method of treating cancer comprising the steps of;

    identifying inhibitory compounds that inhibit both p53-MDM2 and p53-MDMX interactions; and

    administering an effective amount of said inhibitory compound.
14. The method of claim 13, wherein the inhibitory compound is a nucleic acid or polypeptide.
15. The method of claim 13, wherein the inhibitory compound is a dual specific inhibitor of MDM2 and MDMX.
16. The method of claim 13, wherein the inhibitory compound is [SEQ ID NO: 1].

17. The method of claim 13, wherein the inhibitory compound shares at least 85% sequence homology with [SEQ ID NO: 1].

18. The method of claim 14, wherein the nucleic acid encodes a polypeptide having at least 85% sequence homology to [SEQ ID NO: 1].

19. The method of claim 14, wherein the inhibitory compound is identified using a phage display procedure to identify compounds that inhibit p53-MDM2 and p53-MDMX interactions.

20. The method of claim 15, wherein the inhibitory compound is a component of a fusion protein.

21. The method of claim 13, wherein the inhibitory compound is inserted into a virus nucleic acid sequence.

22. The method of claim 21, wherein the virus is an adenovirus.

MDMX selected phages	MDM2 selected phages
T-MX-1: F A P L N R T V E T S P	T-M2-1: Q Q M H L M S Y A P G P
T-MX-2: L T F E H Y W A Q L T S	T-M2-2: T I R P S T T M D S P T
T-MX-3: L T F E H Y W A Q L T S	T-M2-3: Y A N P Q M E K A F E S
T-MX-4: Y A V S S S P R V A A L	T-M2-4: L T F E H Y W A Q L T S
T-MX-5: L T F E H Y W A Q L T S	T-M2-5: L P N L T W A L M P G A
T-MX-6: L T F E H Y W A Q L T S	T-M2-6: Y A N P Q M E K A F A S
T-MX-7: L T F E H Y W A Q L T S	T-M2-7: L T F E H Y W A Q L T S
T-MX-8: L T F E H Y W A Q L T S	T-M2-8: L T F E H Y W A Q L T S
T-MX-9: V V H V P N S A T P P R	T-M2-9: L L A D T T H H R P W T
T-MX-10: L T F E H Y W A Q L T S	T-M2-10: L T F E H Y W A Q L T S

Figure 1.

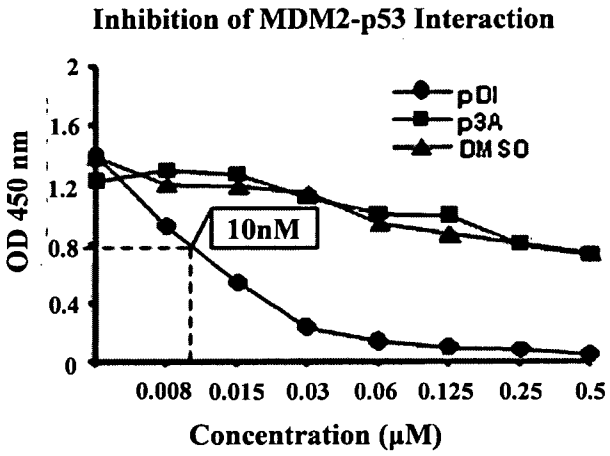

Figure 2.

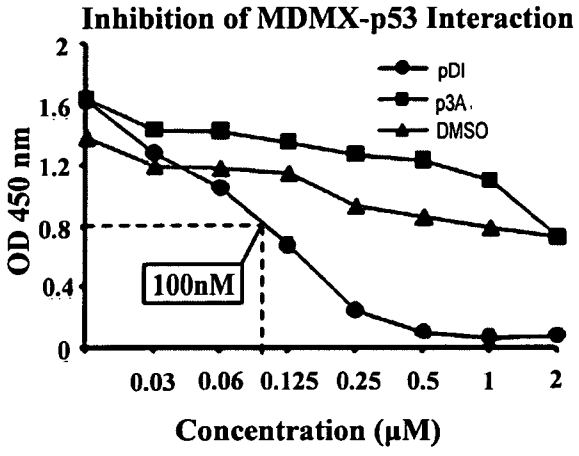

Figure 3.

Peptides (compound)	Sequences	IC_{50} for MDM2 (μmol/L)	IC_{50} for MDMX (μmol/L)
p53pep	QETFSDLWKLLP	3.00	27.50
12/1	MPRFMDYWEGLN	0.15	1.25
Nutlin		0.60	No inhibition
pDI	LTFEHYWAQLTS	0.01	0.10
p3A	LTAEHYAAQATS	No inhibition	No inhibition

Figure 4.

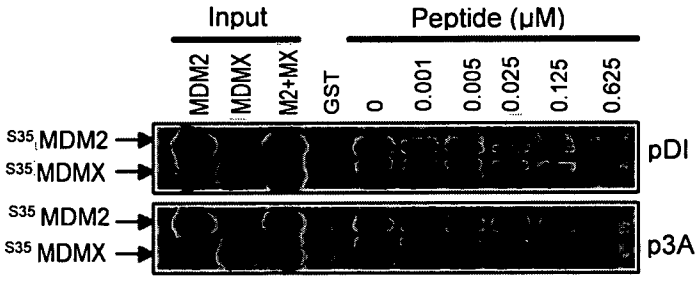

Figure 5.

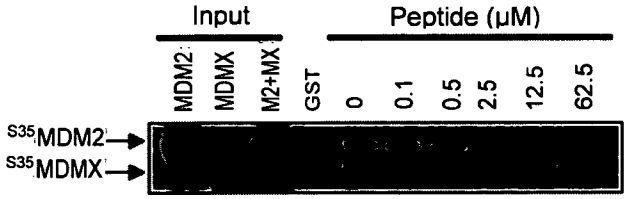

Figure 6.

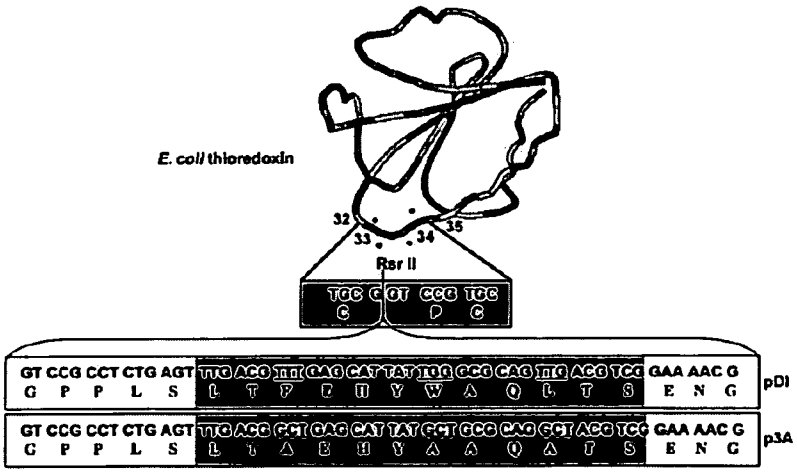

Figure 7.

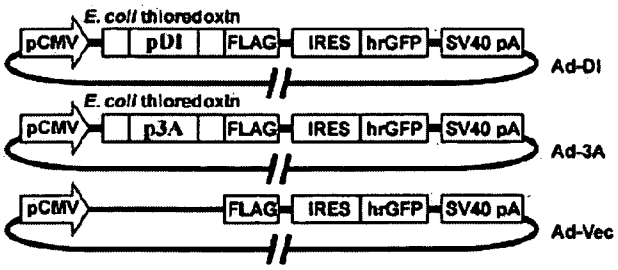

Figure 8.

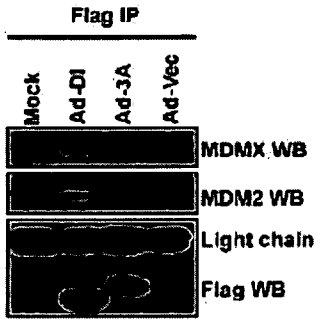

Figure 9.

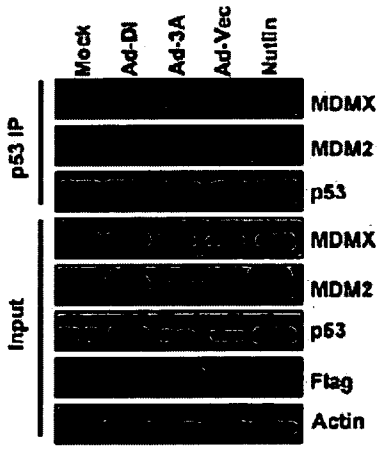

Figure 10.

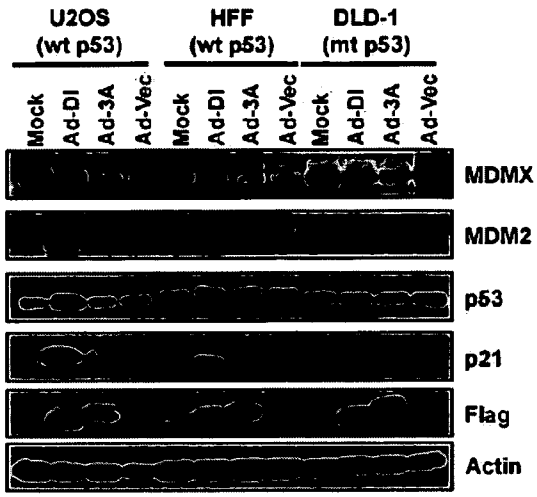

Figure 11.

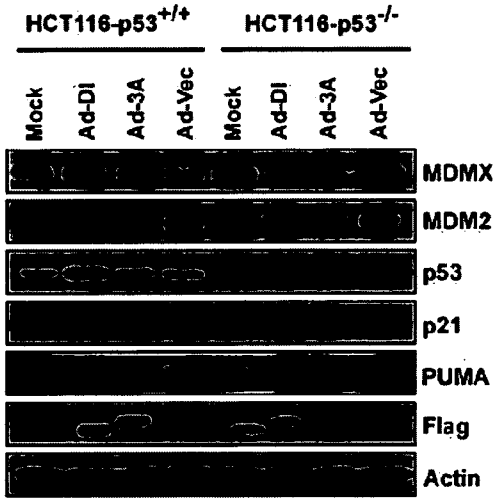

Figure 12.

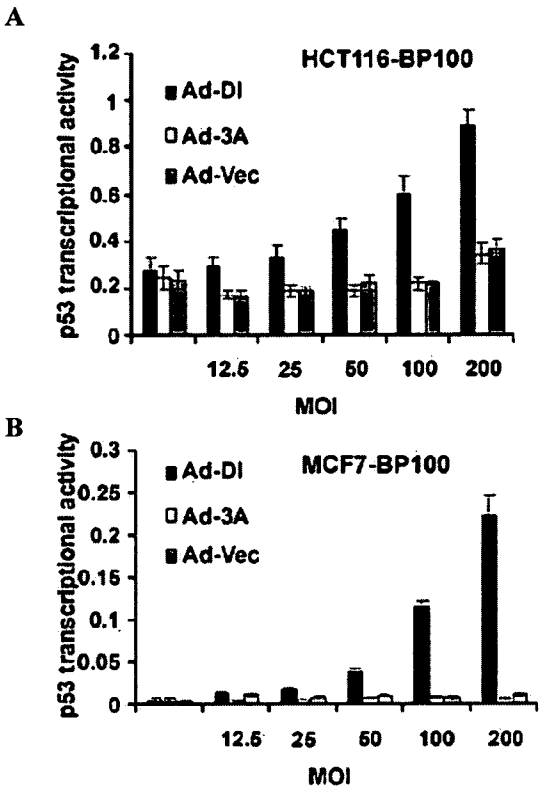
A
HCT116-BP100
Ad-DI
Ad-3A
Ad-Vec
p53 transcriptional activity
1.2
1
0.8
0.6
0.4
0.2
0
12.5
25
50
100
200
MOI
B
MCF7-BP100
Ad-DI
Ad-3A
Ad-Vec
p53 transcriptional activity
0.3
0.25
0.2
0.15
0.1
0.05
0
12.5
25
50
100
200
MOI

Figure 13.

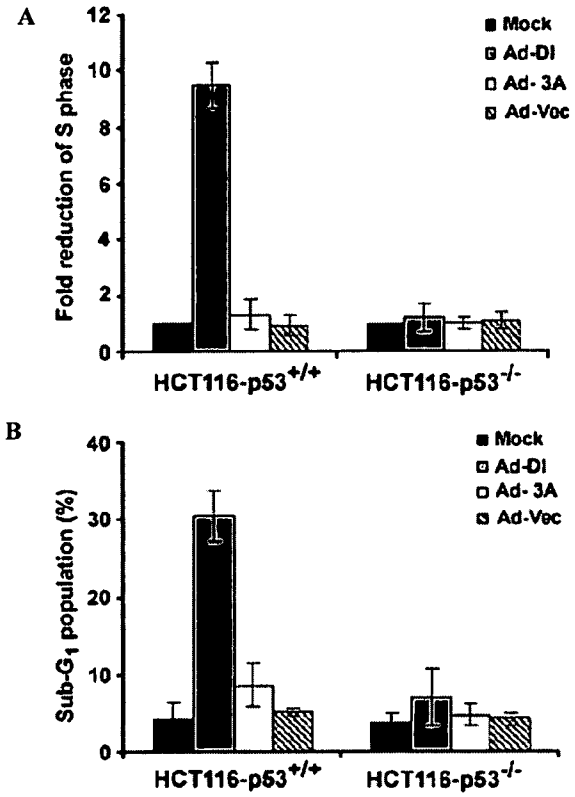

Figure 14.

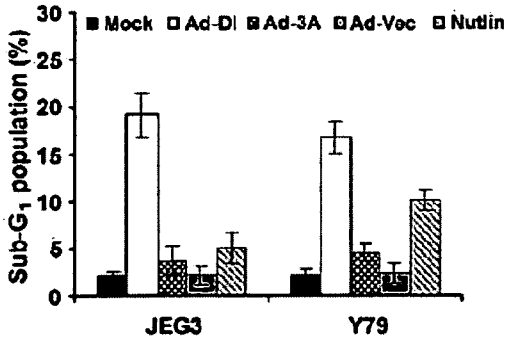

Figure 15.

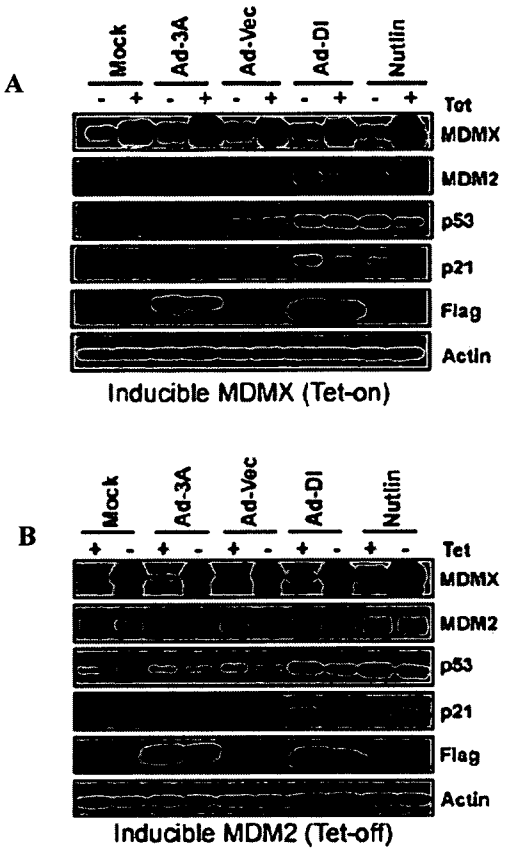

Figure 16.

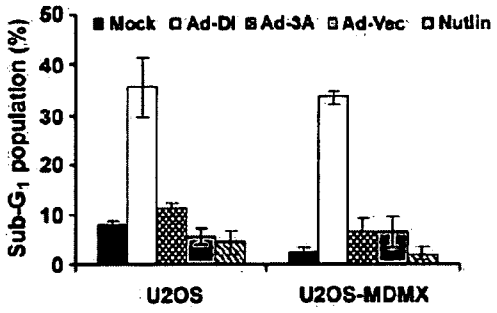

Figure 17.

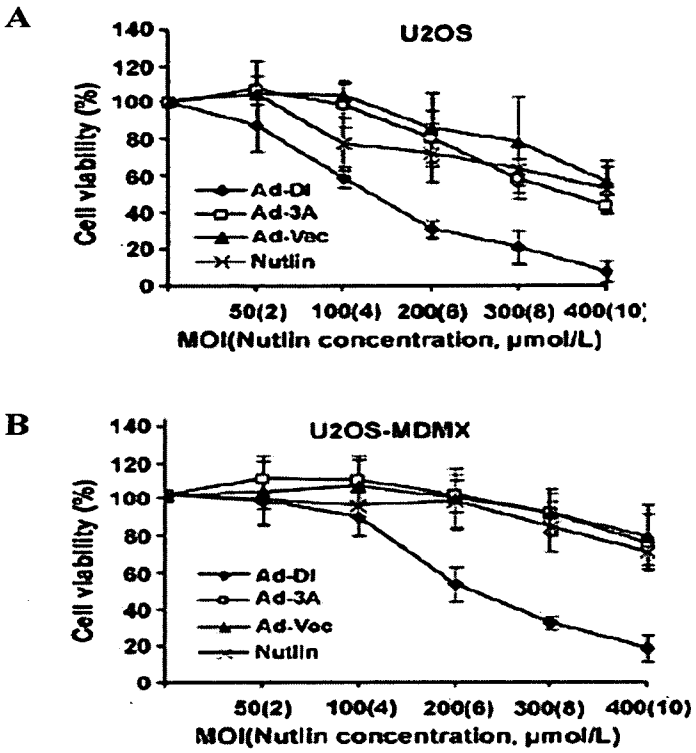

Figure 18.

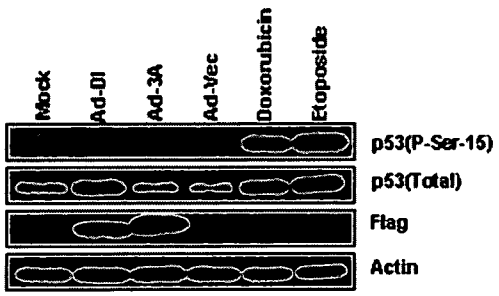

Figure 19.

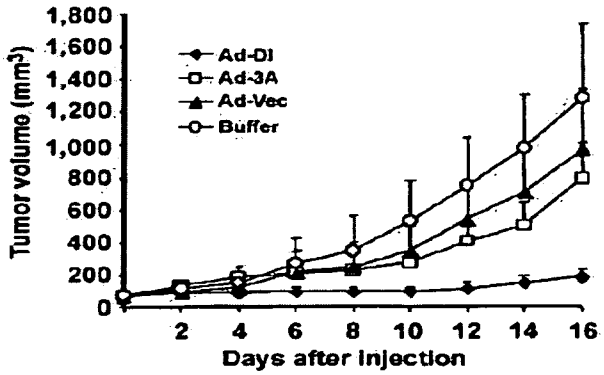

Figure 20.

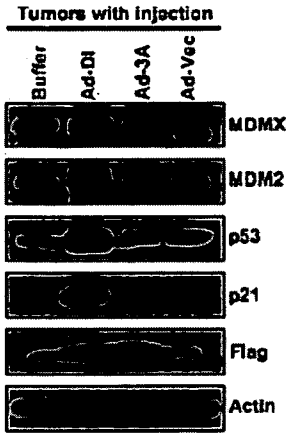

Figure 21.

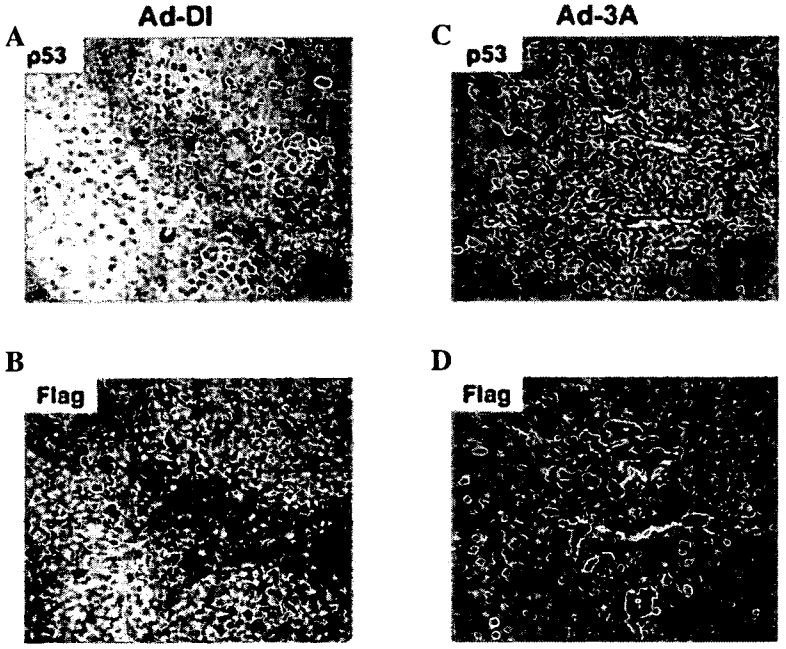

Figure 22.

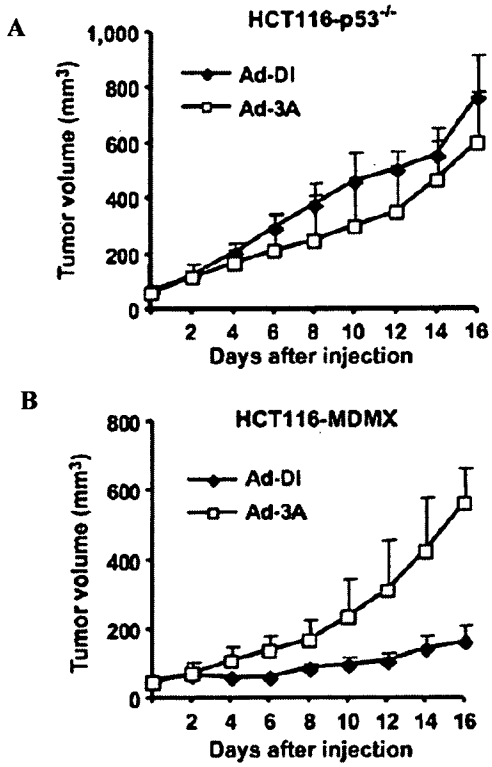
A
HCT116-p53-/-
1,000
800
600
400
200
0
Tumor volume (mm3)
Ad-DI
Ad-3A
2 4 6 8 10 12 14 16
Days after injection
B
HCT116-MDMX
800
600
400
200
0
Tumor volume (mm3)
Ad-DI
Ad-3A
2 4 6 8 10 12 14 16
Days after injection

Figure 23.